Formation of Charge-Transfer Complexes from Neutral Bis(porphyrin) Sandwiches

James P. Collman,* Jonathan L. Kendall, and Judy L. Chen

Department of Chemistry, Stanford University, Stanford, California 94305

K. A. Collins

Department of Physics, Stanford University, Stanford, California 94305

Jean-Claude Marchon*

Département de Recherche Fondamentale sur la Matière Condensée, Service de Chimie Inorganique et Biologique, Laboratoire de Chimie de Coordination (Unité de Recherche Associée au CNRS No. 1194), CEA-Grenoble, 38054 Grenoble, France

Received June 29, 1999

Lanthanide(III) bis(porphyrin) sandwich complexes of octaethyltetraazaporphyrin (OETAP) were synthesized and characterized by UV−vis, IR, and NMR spectroscopies. Cyclic voltammetry results indicate that these neutral sandwich complexes are very easily reduced. Charge-transfer reactions were performed in solution with Ln(OETAP)$_2$ sandwiches and zirconium(IV) bis(porphyrin) sandwiches. The lanthanide sandwiches partially oxidize the zirconium sandwiches in solution, and a solvent dependence of the charge-transfer reaction was observed. The solid-state properties of these charge-transfer materials were also studied. Magnetic susceptibility results suggest weak intermolecular interactions between the sandwiches. The conductivities of the charge-transfer species are greatly improved relative to those of the insulating undoped sandwiches, but the conductivities are in the lower semiconducting region. The low conductivity values are thought to be due to poor intermolecular overlap.

Introduction

Molecular systems in which a donor reduces or partially reduces an acceptor, called charge-transfer materials, have been studied for a number of applications, including molecular conductors and molecular magnets. The special redox properties of bis(porphyrin) sandwich complexes make them interesting candidates for charge-transfer materials. Although partially oxidized porphyrin and phthalocyanine complexes have been investigated previously as charge-transfer materials,[1−6] the partial oxidation was achieved with traditional oxidants such as iodine, nitric acid, or tetracyanoquinone and its derivatives. Bis(porphyrin) sandwich complexes with properly chosen metals and porphyrin ligands, however, allow the formation of charge-transfer complexes in which the porphyrin complexes act as both the electron donor and the electron acceptor.

In porphyrin sandwich complexes, a large metal ion holds two macrocycles closer together than their van der Waals distance of about 3.4 Å.[7−10] As a result, the porphyrin HOMOs overlap to form porphyrin−porphyrin bonding and antibonding orbitals.[11,12] One consequence of this overlap is the raising of the HOMO energy level, which results in a complex that is generally much easier to oxidize than the corresponding monoporphyrin. Thus, the redox properties of porphyrins can be dramatically altered by formation of porphyrin sandwich complexes.

A special class of sandwich complexes with intriguing redox properties can be found among the lanthanide(III) complexes. Neutral bis(porphyrin) lanthanide(III) sandwich complexes have been isolated in two main forms: Ln(Por)$_2$, which is an electron-deficient radical species containing a hole in the porphyrin π system that is delocalized over both porphyrins,[13,14] and Ln(Por)$_2$H, which consists of two porphyrins in their usual −2 oxidation state and a proton that is thought to be bound to the

(1) Ferraro, J. R.; Williams, J. M. *Introduction to Synthetic Electrical Conductors*; Academic Press: Orlando, FL, 1987.
(2) Simon, J.; André, J.-J. *Molecular Semiconductors*; Springer-Verlag: Berlin, 1985.
(3) Capobianchi, A.; Ercolani, C.; Paoletti, A. M.; Pennesi, G.; Rossi, G.; Chiesi-Villa, A.; Rizzoli, C. *Inorg. Chem.* **1993**, *32*, 4605−4611.
(4) Maitrot, M.; Guillaud, G.; Boudjema, B.; André, J.-J.; Strzelecka, H.; Simon, J.; Even, R. *Chem. Phys. Lett.* **1987**, *133*, 59−62.
(5) (a) Ogawa, M. Y.; Martinsen, J.; Palmer, S. M.; Stanton, J. L.; Tanaka, J.; Greene, R. L.; Hoffman, B. M.; Ibers, J. A. *J. Am. Chem. Soc.* **1987**, *109*, 1115−1121. (b) Hoffman, B. M.; Ibers, J. A. *Acc. Chem. Res.* **1983**, *16*, 15−21.
(6) Jiang, J.; Machida, K.-I.; Yamamoto, E.; Adachi, G.-Y. *Chem. Lett.* **1992**, 2427−2430.
(7) Buchler, J. W.; De Cian, A.; Fischer, J.; Kihn-Botulinski, M.; Paulus, H.; Weiss, R. *J. Am. Chem. Soc.* **1986**, *108*, 3652−3659.
(8) Girolami, G. S.; Milam, S. N.; Suslick, K. S. *J. Am. Chem. Soc.* **1988**, *110*, 2011−2012.
(9) Kim, K.; Lee, W. S.; Kim, H.-J.; Cho, S.-H.; Girolami, G. S.; Gorlin, P. A.; Suslick, K. S. *Inorg. Chem.* **1991**, *30*, 2652−2656.
(10) Buchler, J. W.; De Cian, A.; Elschner, S.; Fischer, J.; Hammerschmitt, P.; Weiss, R. *Chem. Ber.* **1992**, *125*, 107−115.
(11) Buchler, J. W.; De Cian, A.; Fischer, J.; Hammerschmitt, P.; Löffler, J.; Scharbert, B.; Weiss, R. *Chem. Ber.* **1989**, *122*, 2219−2228.
(12) Bilsel, O.; Rodriguez, J.; Milam, S. N.; Gorlin, P. A.; Girolami, G. S.; Suslick, K. S.; Holten, D. *J. Am. Chem. Soc.* **1992**, *114*, 6528−6538.
(13) Buchler, J. W.; Scharbert, B. *J. Am. Chem. Soc.* **1988**, *110*, 4272−4276.
(14) Buchler, J. W.; De Cian, A.; Fischer, J.; Kihn-Botulinski, M.; Weiss, R. *Inorg. Chem.* **1988**, *27*, 339−345.

10.1021/ic9907516 CCC: $19.00
Published on Web 03/24/2000

pyrrolic nitrogens.[15,16] (Note that Ln is used to denote a general element of the lanthanide series.) For a given porphyrin, the sandwich complex $Ln(Por)_2$ is much easier to reduce than the corresponding monoporphyrin because of the electron-deficient porphyrin−porphyrin orbital.

The redox potentials of sandwich complexes are also affected greatly by the choice of porphyrin. For example, we have previously compared the effects of octaethylporphyrin (OEP) and octaethyltetraazaporphyrin (OETAP) on the redox potentials of zirconium(IV) porphyrin sandwiches.[17] Although the ligands are structurally similar, OETAP complexes are more easily reduced than the corresponding OEP complexes.[18] The redox potentials of $Zr(OETAP)_2$ are about 0.6 V more positive than the redox potentials of the corresponding OEP complex. Therefore, we speculated that $Ln(OETAP)_2$ complexes should be very easily reduced. We report here the synthesis and characterization of two members of this group, $Gd(OETAP)_2$ and $Lu(OETAP)_2$, and their reduced, protio forms $Gd(OETAP)_2H$ and $Lu(OETAP)_2H$. We also report the synthesis, characterization, conductivity, and magnetic measurements of charge-transfer complexes formed from lanthanide(III) porphyrin sandwich acceptors and zirconium(IV) porphyrin sandwich donors. The degree of charge transfer for each system was controlled by the choice of lanthanide and porphyrin ligands.

Experimental Section

Reagents and Solvents. All solvents and reactants were of reagent grade and were used without further purification, except as indicated below. 1-Chloronaphthalene was dried over 4-Å molecular sieves and then passed through a neutral alumina column prior to use. Dichloromethane, for use in cyclic voltammetry, was dried over magnesium sulfate. Tetrabutylammonium hexafluorophosphate was recrystallized twice from ethanol. $Zr(OEP)_2$,[9] H_2OETAP,[19] $Lu(acac)_3{\cdot}2H_2O$,[20] $Li_2(OETAP)(DME)_2$,[17] and $Zr(OEP)(OETAP)$[17] were synthesized according to literature procedures.

Physical Methods. All manipulations of oxygen- and water-sensitive materials were performed in a Vacuum/Atmosphere Co. nitrogen drybox or in Schlenkware under an argon atmosphere. Oxygen levels in the drybox were monitored with an AO 316-C trace oxygen analyzer and were maintained below 1 ppm. ^{1}H NMR spectra were obtained on a Varian Gemini 200-MHz spectrometer. UV−vis and near-IR spectra were recorded on a Hewlett-Packard 8453 diode array spectrometer. Near-IR and mid-IR spectra were obtained on a Mattson Infinity 60AR spectrometer. Mass spectra and elemental analyses were performed by the Mass Spectrometry Facility of the University of California at San Francisco and by Midwest Microlab, respectively.

Electrochemical studies were performed on an EG&G Princeton Applied Research model 273A potentiostat/galvanostat. The cyclic voltammetry cell contained platinum working and counter electrodes and a silver-wire reference electrode. The sample concentrations were 5×10^{-4} M. The supporting electrolyte was $[NBu_4]^+[PF_6]^-$ (0.1 M). Ferrocene was used as an internal standard.

Conductivity data were recorded as two-probe resistance measurements using a Keithley 160 digital multimeter. Sample pellets were pressed with a KBr hand press, cut to a rectangular geometry, and painted on the sides with silver paint.

Magnetic susceptibility measurements were performed under helium using a Quantum Design MPMS5 SQUID susceptometer at various fields between 100 and 10 000 G. The samples (15−20 mg) were contained in a Kel-F bucket. For each compound, measurements were collected over a temperature range of 2−300 K. Each raw data file was corrected for the diamagnetic contribution of both the sample holder and the compound to the susceptibility. The bucket had been calibrated independently at the same field and temperatures. The values of the diamagnetic susceptibilities of the free-base porphyrins measured in earlier work from these laboratories (H_2OEP, -481×10^{-6} emu/mol; H_2OETAP, -431×10^{-6} emu/mol),[21] along with diamagnetic correction factors for the metals given in the literature,[22] were used to calculate the total diamagnetic correction factors for the porphyrin sandwiches ($[Gd(OETAP)_2]$, -880×10^{-6} emu/mol; $[Zr(OEP)_2]^+[Gd(OETAP)_2]^-$, -1740×10^{-6} emu/mol). The experimental data were fit using a locally written Fortran program[23] that effects matrix diagonalization for an interaction Hamiltonian $H = -JS_1S_2$ with $S_1 = {}^7/_2$ and $S_2 = {}^1/_2$.

X-ray measurements were performed on a Rigaku D-Max automated powder diffractometer. Samples were placed on a silica glass holder and scanned over 2Θ values ranging from 5° to 50° with a step size of 0.05° using Cu Kα radiation and a graphite monochromator.

Synthesis

$Gd(OETAP)_2H$. In a nitrogen box, a 100-mL round-bottom flask was filled with 206 mg (0.285 mmol) of $Li_2OETAP(DME)_2$, 70 mg (0.143 mmol) of $Gd(acac)_3{\cdot}2H_2O$, and 15 mL of 1-chloronaphthalene. The solution was heated at reflux for 6 h and cooled to room temperature, and the flask was removed from the box. The solvent was removed by vacuum distillation. The product was separated on a silica column using 2:1 hexanes:toluene to elute traces of $Gd(OETAP)_2$ as the first (blue/purple) band and unreacted H_2OETAP as the second (purple) band. A 1:1 mixture of hexanes:toluene was used to elute the product as the third (blue) band. The solvent was removed under vacuum. A mass of 133 mg (0.108 mmol) of product was collected (76% yield). UV−vis (CH_2Cl_2) λ_{max} (log ϵ): 328 (Soret) (5.02), 453 (3.99), 596 (4.92) nm. MS (LSIMS) *m/e*: 1231.4; calcd M^+ for $C_{64}H_{81}GdN_{16}$, 1231.6. IR (KBr, cm^{-1}): 3403 (s), 2964 (s), 2933 (s), 2872 (s), 1461 (s), 1373 (w), 1261 (w), 1149 (m), 1058 (w), 1009 (m), 950 (s), 903 (w), 767 (w), 742 (w), 668 (w). Elemental anal. Calcd for $C_{64}H_{81}GdN_{16}$: 62.41% C, 6.63% H, 18.19% N. Found: 62.56% C, 6.68% H, 17.96% N.

$Gd(OETAP)_2$. A 25-mL round-bottom flask was filled with 8 mg (6.5 μmol) of $Gd(OETAP)_2H$ and 2 mL of dichloromethane. A solution of 0.75 mg (3.25 μmol) of dichlorodicyanobenzoquinone (DDQ) in 1 mL of dichloromethane was added dropwise to the reaction flask over a 2 min period. The solution was stirred for 5 min. The solvent was removed under vacuum. The product was separated on a silica column using 2:1 hexanes:toluene as the eluent. The first (blue/purple) band was collected as the product. A mass of 7.8 mg (6.4 μmol) of product was collected (98% yield). The compound was crystallized by slow evaporation of a dichloromethane/acetonitrile solution. UV−vis (CH_2Cl_2) λ_{max} (log ϵ): 317 (Soret) (5.15), 485, 592 (4.72), 702 (3.21), 784 (3.31), 918 (3.00) nm. Near-IR (CCl_4) λ_{max} (log ϵ): 1740 (4.02) nm. MS (LSIMS) *m/e*: 1231.4; calcd MH^+ for $C_{64}H_{80}GdN_{16}$, 1231.6. IR (KBr, cm^{-1}): 2965 (s), 2934 (s), 2872 (s), 1610 (w), 1461 (m), 1343 (s), 1315 (m), 1261 (w), 1125 (m), 1056 (w), 1011 (s), 948 (s), 648 (m). Elemental anal. Calcd for $C_{64}H_{80}GdN_{16}$: 62.46% C, 6.55% H, 18.21% N. Found: 62.50% C, 6.58% H, 18.28% N.

$Lu(OETAP)_2H$ and $Lu(OETAP)_2$. In a nitrogen box, a 100-mL flask was filled with 157 mg (0.217 mmol) of $Li_2OETAP(DME)_2$, 53 mg (0.109 mmol) of $Lu(acac)_3{\cdot}2H_2O$, and 10 mL of 1-chloronaphthalene. The solution was heated at reflux for 4 h. The reaction mixture

(15) Buchler, J. W.; Kihn-Botulinski, M.; Löffler, J.; Scharbert, B. *New J. Chem.* **1992**, *16*, 545−553.
(16) (a) Spyroulias, G. A.; Coutsolelos, A. G. *Inorg. Chem.* **1996**, *35*, 1382−1385. (b) Spyroulias, G. A.; Coutsolelos, A. G.; Raptopoulou, C. P.; Terzis, A. *Inorg. Chem.* **1995**, *34*, 2476−2479. (c) See Supporting Information for spectra of $Gd(OETAP)_2$ and $Gd(OETAP)_2H$.
(17) Collman, J. P.; Kendall, J. L.; Chen, J. L.; Eberspacher, T. A.; Moylan, C. R. *Inorg. Chem.* **1997**, *36*, 5603−5608.
(18) Fitzgerald, J. P.; Haggerty, B. S.; Rheingold, A. L.; May, L.; Brewer, G. A. *Inorg. Chem.* **1992**, *31*, 2006−2013.
(19) Fitzgerald, J.; Taylor, W.; Owen, H. *Synthesis* **1991**, 686.
(20) Stites, J. G.; McCarty, C. N.; Quill, L. L. *J. Am. Chem. Soc.* **1948**, *70*, 3142−3143.
(21) Arnold Godwin, H.; Collman, J. P.; Marchon, J.-C.; Maldivi, P.; Yee, G. T.; Conklin, B. J. *Inorg. Chem.* **1997**, *36*, 3499−3502. The value $\chi_M = -470 \times 10^{-6}$ emu/mol ($\pm 10 \times 10^{-6}$ emu/mol) for H_2OEP was reported previously: Lueken, H.; Buchler, J. W.; Lay, K. L. *Z. Naturforsch.* **1976**, *31b*, 1596−1603.
(22) Carlin, R. L. *Magnetochemistry*; Springer-Verlag: Berlin, 1986.
(23) Cheng, B.; Cukiernik, F.; Fries, P. H.; Marchon, J.-C.; Scheidt, W. R. *Inorg. Chem.* **1995**, *34*, 4627−4639.

was cooled to room temperature, and the flask was removed from the box. The solvent was removed by vacuum distillation, and the product was separated on a silica column using 2:1 hexanes:toluene as the eluent. The first band was collected as $Lu(OETAP)_2$ (33 mg, 0.026 mmol, 24% yield), and the second band was collected as $Lu(OETAP)_2H$ (62 mg, 0.030 mmol, 46% yield).

Lu(OETAP)$_2$H. UV−vis (CH_2Cl_2) λ_{max} (log ϵ): 325 (4.90), 463 (4.03), 599 (4.74) nm. ^{1}H NMR (C_6D_6): δ 4.14 (m, 16H), 3.73 (m, 16H), 1.81 (m, 48H), −8.60 (s, 1H). MS (LSIMS) *m*/*e*: 1249.4; calcd M^+ for $C_{64}H_{81}LuN_{16}$, 1248.6. IR (KBr, cm^{-1}): 3403 (m), 2963 (s), 2931 (s), 2869 (s), 1474 (s), 1463 (s), 1435 (s), 1428 (s), 1419 (s), 1374 (w), 1261 (w), 1149 (m), 1058 (w), 1009 (m), 953 (s), 946 (s), 904 (w), 874 (w), 759 (w), 706 (w).

Lu(OETAP)$_2$. UV−vis (CH_2Cl_2) λ_{max} (log ϵ): 315 (5.03), 496 (3.91), 585 (4.61), 707 (3.22), 786 (3.42) nm. Near-IR (CCl_4) λ_{max} (log ϵ): 1460 (3.96) nm. MS (LSIMS) *m*/*e*: 1249.4; calcd MH^+ for $C_{64}H_{80}LuN_{16}$, 1248.6. IR (KBr, cm^{-1}): 2964 (s), 2932 (s), 2871 (s), 1461 (m), 1453 (m), 1405 (m), 1353 (s), 1317 (m), 1261 (m), 1126 (m), 1056 (m), 1014 (s), 950 (s), 771 (m), 650 (m). Elemental anal. Calcd for $C_{64}H_{80}LuN_{16}$: 61.57% C, 6.46% H, 17.95% N. Found: 60.84% C, 6.50% H, 17.18% N.

Lu(OETAP)$_2$. A 25-mL round-bottom flask was filled with 30 mg (0.024 mmol) of $Lu(OETAP)_2H$ and 2 mL of dichloromethane. To this solution was added 2.8 mg (0.012 mmol) of DDQ in 2 mL of dichloromethane. The solution was stirred for 10 min, and the solvent was removed under vacuum. The product was separated on a silica column using 2:1 hexanes:toluene as the eluent. The first (blue/purple) band was collected as the product. A mass of 28 mg (0.022 mmol) of product was collected (92% yield). The characterization data for this compound were identical to those for $Lu(OETAP)_2$, as described above.

[Zr(OEP)$_2$][Gd(OETAP)$_2$]. For solid-state studies of the charge-transfer system, equimolar amounts of $Gd(OETAP)_2$ and $Zr(OEP)_2$ were dissolved in a minimum amount of dichloromethane. An amount of acetonitrile equal to approximately twice the solution volume was layered over the dichloromethane solution. The solvents were allowed to mix slowly via diffusion, and about one-third of the solvent was allowed to evaporate over several days. The crystals were filtered, washed with acetonitrile, and dried under vacuum. Calcd for 1:1 $Zr(OEP)_2$:$Gd(OETAP)_2$ = $C_{136}H_{168}GdN_{24}Zr$: 68.42% C, 7.09% H, 14.08% N. Found: 68.28% C, 7.13% H, 14.29% N.

[Zr(OEP)$_2$][Lu(OETAP)$_2$]. In a similar manner to that described above, crystals of $[Zr(OEP)_2][Lu(OETAP)_2]$ were grown from dichloromethane/acetonitrile and were dried under vacuum. Calculated for 1:1 $Zr(OEP)_2$:$Lu(OETAP)_2$ = $C_{136}H_{168}LuN_{24}Zr$: 67.92% C, 7.04% H, 13.98% N. Found: 67.37% C, 6.95% H, 14.20% N.

Results and Discussion

Synthesis and Characterization. $Gd(OETAP)_2H$ and $Lu(OETAP)_2H$ were synthesized by the reaction of dilithium octaethyltetraazaporphyrin with the corresponding lanthanide(III) acetylacetonate in refluxing 1-chloronaphthalene. No product was observed when solvents with lower boiling points were used. After column chromatography on silica, $Gd(OETAP)_2H$ was isolated in a 76% yield, along with traces of $Gd(OETAP)_2$. In contrast, the reaction with lutetium(III) acetylacetonate produced a 46% yield of the reduced, protio form of the sandwich complex and a 24% yield of the π-radical form. The reduced compounds were easily converted, in quantitative yield, to the π-radical species upon reaction with DDQ.

Although $Gd(OETAP)_2$, $Lu(OETAP)_2$, $Gd(OETAP)_2H$, and $Lu(OETAP)_2H$ are all stable in solution when exposed to atmospheric conditions, we believe that at least some of the π-radical complexes obtained in the synthesis of the reduced forms were generated during the chromatography step. Under the chromatographic conditions, purified $Lu(OETAP)_2H$ was partially converted to the π-radical form $Lu(OETAP)_2$. When thin-layer chromatography was performed on $Lu(OETAP)_2H$ in the drybox, $Lu(OETAP)_2$ was not observed. Although solutions of $Lu(OETAP)_2H$ are stable to air, air oxidation of this compound is greatly facilitated by silica. The greater air tolerance of $Gd(OETAP)_2H$ on silica compared to that of $Lu(OETAP)_2H$ is not surprising, considering that $Lu(OETAP)_2$ is about 142 mV harder to reduce than $Gd(OETAP)_2$ (vide infra).

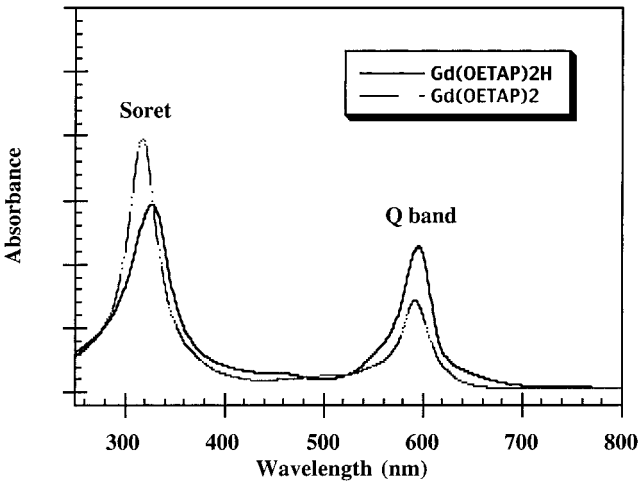

Figure 1. UV−vis spectrum of $Gd(OETAP)_2H$ and $Gd(OETAP)_2$ in dichloromethane.

Despite repeated attempts, we were unable to grow crystals of either $Lu(OETAP)_2H$ or $Lu(OETAP)_2$. Such a purification step was necessary to obtain suitable elemental analysis for $Gd(OETAP)_2$ [though not for $Gd(OETAP)_2H$]. Thus, we were unable to obtain acceptable elemental analyses for either of the lutetium species. However, we were able to grow crystals of the charge-transfer complex $[Zr(OEP)_2][Lu(OETAP)_2]$, and we obtained an acceptable elemental analysis consistent with the proposed composition.

The spectra of $Gd(OETAP)_2H$ and $Gd(OETAP)_2$ are shown in Figure 1. The UV−vis spectra of the π-radical and reduced sandwich complexes are similar in appearance with two exceptions. First, the Q band is more intense and the Soret band is less intense for $Ln(OETAP)_2H$ compared to the corresponding bands for $Ln(OETAP)_2$. Second, the Soret bands for the π-radical species are blue-shifted by 10−11 nm compared to the corresponding bands for the reduced forms. This blue shift has been observed for other lanthanide sandwich complexes.[24]

A characteristic of π-radical porphyrin complexes is the presence of a broad, moderately intense ($\epsilon \approx 10\,000\ M^{-1}\ cm^{-1}$) near-IR band that corresponds to a transition from the porphyrin−porphyrin bonding orbital to the porphyrin−porphyrin antibonding orbital. For a given ligand, the porphyrins are held closer together as the metal radius decreases,[13] resulting in increased interaction between the two porphyrin rings and a larger splitting of the porphyrin−porphyrin bonding and antibonding orbitals.[25] The near-IR band occurs at 1460 nm (6849 cm^{-1}) for $Lu(OETAP)_2$ and at 1740 nm (5747 cm^{-1}) for $Gd(OETAP)_2$ in CCl_4. Because Lu(III) has an ionic radius of 0.97 Å and Gd(III) has an ionic radius of 1.06 Å,[26] the Lu(III) complex has the higher-energy band. Because the reduced

(24) Buchler, J. W.; Kihn-Botulinski, M.; Löffler, J.; Scharbert, B. *New J. Chem.* **1992**, *16*, 545−553.
(25) (a) Donohoe, R. J.; Duchowski, J. K.; Bocian, D. F. *J. Am. Chem. Soc.* **1988**, *110*, 6119−6124. (b) Duchowski, J. K.; Bocian, D. F. *J. Am. Chem. Soc.* **1990**, *112*, 3312−3318. (c) Duchowski, J. K.; Bocian, D. F. *Inorg. Chem.* **1990**, *29*, 4158−4160. (d) Perng, J.-H.; Duchowski, J. K.; Bocian, D. F. *J. Phys. Chem.* **1990**, *94*, 6684−6691.
(26) Shannon, R. D.; Prewitt, C. T. *Acta Crystallogr.* **1969**, *B25*, 925−946.

Table 1. Cyclic Voltammetry Results for Sandwich Complexes[a]

	E_1 (mV)	E_2 (mV)
$Gd(OETAP)_2$	648	105
$Lu(OETAP)_2$	591	−37
$Zr(OEP)_2$	−2	
Zr(OEP)(OETAP)	242	

[a] Data were collected in CH_2Cl_2 using tetrabutylammonium hexafluorophosphate as a supporting electrolyte. Results are given vs Ag/AgCl using Cp_2Fe(III/II) as an internal standard (see ref 28).

species have a filled porphyrin−porphyrin antibonding orbital, they do not exhibit this near-IR absorption.

IR spectroscopy further distinguishes the π-radical and reduced forms of the sandwich complexes. The protonated, reduced forms show N−H stretches, which are absent in the π-radical forms. $Gd(OETAP)_2H$ and $Lu(OETAP)_2H$ exhibit N−H stretches at 3403 cm^{-1}, which lie about 100 cm^{-1} higher in energy than the N−H stretch for H_2OETAP (3295 cm^{-1}) and the N−H stretches for $La(OEP)_2H$[24] and $Sm(OEP)_2H$.[16c]

IR "marker" bands are exhibited by monoporphyrin cation radicals[27] and π-radical sandwich complexes.[24] We have previously identified the octaethyltetraazaporphyrin radical marker band in the region of 1325−1310 cm^{-1}.[17] $Gd(OETAP)_2$ and $Lu(OETAP)_2$ show characteristic marker bands at 1315 and 1317 cm^{-1}, respectively, consistent with octaethyltetraazaporphyrin π-radicals. As expected, $Gd(OETAP)_2H$ and $Lu(OETAP)_2H$ do not show bands in this region.

The ^1H NMR spectrum of $Lu(OETAP)_2H$ was taken in $CDCl_3$. The general appearance of the spectrum is similar to that of the NMR spectra of sandwich porphyrin complexes. The diastereotopic methylene signals occur between 3.66 and 4.21 ppm, and the methyl group has a shift of 1.81 ppm. The N−H proton appears as a singlet at −8.60 ppm, which is consistent with a proton residing on the pyrrolic nitrogens.[16a,24] The N−H proton in $Lu(TPP)_2H$ (TPP = tetraphenylporphyrin) in $CDCl_3$ was found to appear as a singlet at −8.73 ppm.[16a]

Cyclic Voltammetry. The first oxidation (E_1) and reduction (E_2) potentials of the lanthanide sandwich complexes in CH_2Cl_2 were measured by cyclic voltammetry.

$$Ln(OETAP)_2^+ + e^- = Ln(OETAP)_2 \quad E_1$$

$$Ln(OETAP)_2 + e^- = Ln(OETAP)_2^- \quad E_2$$

The values of these reversible redox couples are given in Table 1, along with the oxidation potentials (E_1) of two zirconium sandwich complexes.

$$Zr(Por)_2^+ + e^- = Zr(Por)_2 \quad E_1$$

The $Ln(OETAP)_2$ complexes are quite easily reduced. The lutetium(III) sandwich complex is 142 mV harder to reduce than the gadolinium(III) sandwich complexes. The differences in the oxidation and reduction potentials of the Gd(III) and Lu(III) sandwich complexes result from the smaller lutetium(III) ion holding the porphyrins closer together. In the Lu(III) sandwich, the porphyrin rings interact more strongly, raising the energy of the partially occupied redox-active orbital and making the compound harder to reduce and easier to oxidize. This trend was also observed in $Ln(OEP)_2$ sandwich complexes; for example, $Gd(OEP)_2$ is 100 mV easier to reduce and 80 mV harder to oxidize than $Lu(OEP)_2$.[13]

(27) Shimomura, E. T.; Phillippi, M. A.; Goff, H. M.; Scholz, W. F.; Reed, C. A. *J. Am. Chem. Soc.* **1981**, *103*, 6778−6780.

Table 2. Differences in Redox Potentials for Three Charge-Transfer Systems and the Calculated Equilibrium Constants

system	$E_{2(acceptor)} - E_{1(donor)}$ (mV)	K_{eq}	% transfer
$Zr(OEP)_2/Gd(OETAP)_2$	107	65	89%
$Zr(OEP)_2/Lu(OETAP)_2$	−35	0.26	34%
$Zr(OEP)(OETAP)/Gd(OETAP)_2$	−137	0.0048	6%

Table 3. Solution Charge-Transfer Reactions of $Ln(OETAP)_2$ and $Zr(Por)_2$ Complexes[a]

donor/acceptor	solvent system	% transfer
$Zr(OEP)_2/Gd(OETAP)_2$	pentane	4 ± 2%
	CH_2Cl_2	26 ± 3%
	$CH_2Cl_2 + TBAPF_6$	79 ± 7%
	CH_3CN[b]	85 ± 7%
$Zr(OEP)_2/Lu(OETAP)_2$	CH_2Cl_2	6 ± 2%
	$CH_2Cl_2 + TBAPF_6$	26 ± 1%
$Zr(OEP)(OETAP)/Gd(OETAP)_2$	CH_2Cl_2	3 ± 1%
	$CH_2Cl_2 + TBAPF_6$	9 ± 6%
	CH_3CN[b]	21 ± 3%

[a] Results are averages of several repeated measurements. [b] Dichloromethane (5%) was added to dissolve the neutral sandwiches, which are insoluble in CH_3CN.

The values of the first reduction potentials (E_2) of the lanthanide(III) complexes are similar to the values of the first oxidation potentials (E_1) of the zirconium(IV) complexes, which indicates that partial charge transfer should occur between these species. The degree of charge transfer between the zirconium(IV) donor complexes (D) and lanthanide(III) acceptor complexes (A) under the conditions used in electrochemistry can be estimated using the Nernst equation, the first oxidation potentials of the zirconium complexes, and the first reduction potentials of the lanthanide complexes.

$$D + A \rightleftharpoons D^+ A^-$$

$$\log K_{eq} = [E_{2(acceptor)} - E_{1(donor)}]/0.059 \text{ V}$$

The calculated equilibrium constants and degrees of charge transfer for three systems using the electrochemical data are shown in Table 2.

Solution Charge-Transfer Studies. The three charge-transfer systems shown in Table 2 were studied in solution. Near-IR spectroscopy provides a convenient method of determining the degree of charge transfer, as near-IR bands appear in the π-radical form of both the donor and the acceptor sandwiches. These bands are reasonably strong ($\epsilon \geq 10\,000$ M^{-1} cm^{-1}) and are not significantly affected by the absorptions of any other species present in the reaction ($\epsilon < 1000$ M^{-1} cm^{-1}). The degree of charge transfer in solution was calculated using the absorptions at the near-IR wavelengths for D^+ {960 nm for $[Zr(OEP)_2]^+$ and 999 nm for $[Zr(OEP)(OETAP)]^+$}[9,17] and A [1740 nm for $Gd(OETAP)_2$ and 1460 nm for $Lu(OETAP)_2$], the known concentrations of the starting neutral D and A, and the extinction coefficients of all four species (D, A, D^+, and A^-) at the wavelengths of interest. The results of the charge-transfer reactions in various solvents are presented in Table 3.

The solvent affected the degree of charge transfer in the reaction. A greater degree of charge transfer was observed in more polar solvents, which stabilize the ions formed in the charge-transfer reaction and shift the equilibrium toward the products. Interestingly, no precipitate was observed in any of the charge-transfer reactions studied. The neutral sandwiches (reactants) are very soluble in both chlorinated and hydrocarbon solvents, but the ionic species (products) are less soluble in nonpolar solvents. For example, $[Zr(OEP)_2]^+[SbCl_6]^-$ is in-

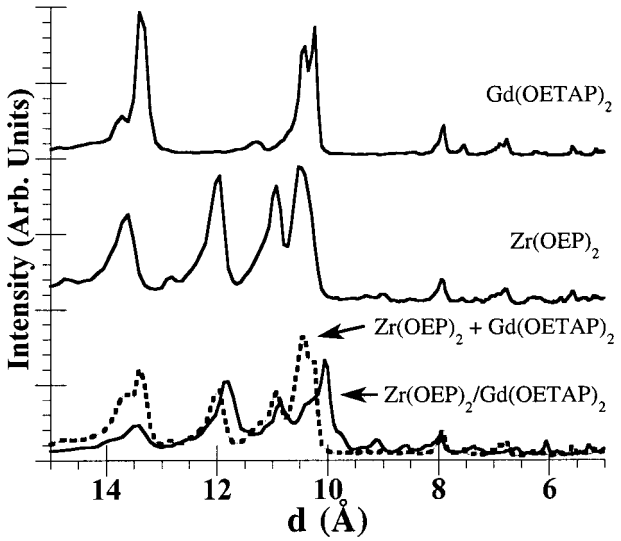

Figure 2. X-ray powder patterns of $Gd(OETAP)_2$ (top), $Zr(OEP)_2$ (middle), and $[Zr(OEP)_2][Gd(OETAP)_2]$ and $[Zr(OEP)_2]+[Gd(OETAP)_2]$ (bottom).

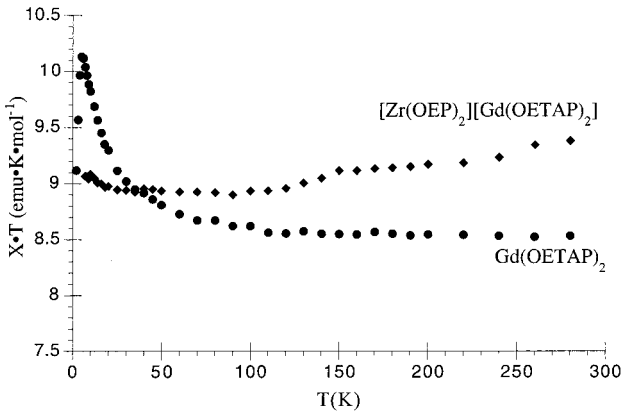

Figure 3. Solid circles represent the temperature dependence of $\chi_M T$ for $Gd(OETAP)_2$, which can be fit with the following values of the adjustable parameters: $J = +1.9\ cm^{-1}$, $g = 1.991$, and $TIP = -8.3 \times 10^{-4}\ cm^3\ K\ mol^{-1}$. Solid diamonds represent the temperature dependence of $\chi_M T$ for $[Zr(OEP)_2][Gd(OETAP)_2]$.

soluble in hydrocarbons.[9] Although the products are less soluble than the reactants in pentane, the equilibrium favors the reactants, and no precipitate is formed. The more polar solvents are effective at stabilizing the products, and the equilibrium shifts toward completion. The ionic products are more soluble in the polar solvents, and no precipitate is formed.

For a comparison of the observed and predicted charge-transfer values, the reactions were also performed in the presence of tetrabutylammonium hexafluorophosphate ($TBAPF_6$) in dichloromethane to mirror the electrochemical conditions under which the oxidation and reduction potentials were obtained. When the reactions were performed under the electrochemical conditions, the values for the observed charge-transfer reactions were consistent with the predicted values.

Solid State Studies. Magnetic and conducting properties were performed on crystals grown by slow evaporation of dichloromethane/acetonitrile solutions of the corresponding donor and acceptor molecules. The crystals were polycrystalline and were shown to be 1:1 adducts by elemental analysis. X-ray-quality single crystals did not result from this or any other crystallization method.

X-ray Powder Diffraction. X-ray powder diffraction patterns were obtained for polycrystalline samples of $[Zr(OEP)_2][Gd(OETAP)_2]$, $Zr(OEP)_2$, and $Gd(OETAP)_2$. The three patterns are compared in Figure 2, along with a simulated pattern of $Zr(OEP)_2 + Gd(OETAP)_2$. The data clearly show that $[Zr(OEP)_2][Gd(OETAP)_2]$ is not a mechanical mixture of the two components, $Zr(OEP)_2$ and $Gd(OETAP)_2$, but has a unique structure.

Magnetic Studies. $Gd(OETAP)_2$ contains an $S = {}^7/_2$ Gd(III) center and an $S = {}^1/_2$ π-radical delocalized over the two porphyrins in the sandwich. Its molar magnetic susceptibility, χ_M, in the temperature range of 2−300 K was measured at several values of the magnetic field strength between 100 and 10 000 G. A plot of the temperature dependence of $\chi_M T$ for $Gd(OETAP)_2$ in a field of 500 G is shown in Figure 3. At room temperature, $\chi_M T$ is equal to 8.5 $cm^3\ K\ mol^{-1}$. When the temperature is lowered, $\chi_M T$ first remains constant until 100 K, then increases to a maximum value of 10 $cm^3\ K\ mol^{-1}$ at 5 K, and then eventually decreases at temperatures below 5 K. This behavior is typical of a ferromagnetic Gd(III)−porphyrin radical interaction. The data were fit to the interaction Hamiltonian $H = -JS_1S_2$ of an $S_1 = {}^7/_2$ and $S_2 = {}^1/_2$ spin pair, including a temperature-independent paramagnetism (TIP) term. A satisfactory fit for the temperature range of 5−300 K was obtained with the adjustable parameters $J = +1.9\ cm^{-1}$, $g = 1.991$, and $TIP = -8.3 \times 10^{-4}\ cm^3\ K\ mol^{-1}$.

In $[Zr(OEP)_2][Gd(OETAP)_2]$, the porphyrins at the Gd(III) center have lost their π-radical character, and the sandwich is anionic. The electron hole has been transferred to the Zr(IV) porphyrin sandwich, which has become a π-radical cation. The molar magnetic susceptibility χ_M of this complex in the temperature range of 7−300 K was measured at several values of magnetic field between 500 and 10 000 G. A plot of the temperature dependence of $\chi_M T$ for $[Zr(OEP)_2][Gd(OETAP)_2]$ in a field of 500 G is shown in Figure 3. In the range from room temperature down to about 7 K, $\chi_M T$ is nearly constant and equal to 9.1−9.4 $cm^3\ K\ mol^{-1}$. This Curie-like behavior in the temperature range of 7−300 K indicates noninteracting spins in the solid lattice.

Several examples of compounds that contain an $S = {}^1/_2$ spin in the proximity of an $S = {}^7/_2$ Gd(III) center have been described recently.[29−32] In these compounds, the $S = {}^1/_2$ spin is either a Cu(II) ion or a delocalized nitroxide-type ligand. The question that has been addressed in these studies is the nature of the magnetic interaction between the two spins: is it ferromagnetic or antiferromagnetic? Pioneering work by Gatteschi et al.[29] has shown that in trinuclear Cu(II)Gd(III)Cu(II) complexes, the Gd(III)−Cu(II) interaction is ferromagnetic, irrespective of the details of the molecular structure that encompasses the $S = {}^7/_2$ and $S = {}^1/_2$ spins. Similar results have been obtained by Gatteschi and Rey with a discrete complex in which a Gd(III) center is coordinated by two nitronylnitroxide ligands: this three-spin system exhibits weak ferromagnetic coupling between the $S = {}^7/_2$ gadolinium(III) center and the $S = {}^1/_2$ radicals.[30] The ferromagnetic nature of the Gd(III)−Cu(II) pair in three binuclear Gd(III)−Cu(II) complexes was later confirmed by Matsumoto et al.[31] A general interpretation [in terms of the contraction of the 4f magnetic orbitals of the Gd(III) center] of

(28) Kelly, S. L.; Kadish, K. M. *Inorg. Chem.* **1984**, *23*, 679−687.
(29) Bencini, A.; Benelli, C.; Caneschi, A.; Carlin, R. L.; Dei, A.; Gatteschi, D. *J. Am. Chem. Soc.* **1985**, *107*, 8128−8136.
(30) Benelli, C.; Caneschi, A.; Gatteschi, D.; Pardi, L.; Rey, P.; Shum, D. P.; Carlin, R. L. *Inorg. Chem.* **1989**, *28*, 272−275.
(31) Sakamoto, M.; Hashimura, M.; Matsuki, K.; Matsumoto, N.; Inoue, K.; Okawa, H. *Bull. Chem. Soc. Jpn.* **1991**, *64*, 3639−3641.
(32) Andruh, M.; Ramade, I.; Codjovi, E.; Guillou, O.; Kahn, O.; Trombe, J. C. *J. Am. Chem. Soc.* **1993**, *115*, 1822−1829.

Table 4. Two-Probe Conductivity Data for Charge-Transfer Systems and Their Comparison to the $Gd(OETAP)_2$ and $Zr(OEP)_2$ Complexes

system	conductivity (Ω^{-1} cm^{-1})	E_{act} (eV)
$[Zr(OEP)_2][Gd(OETAP)_2]$	$5-8 \times 10^{-5}$	0.40
$[Zr(OEP)_2][Lu(OETAP)_2]$	$0.6-1 \times 10^{-5}$	0.43
$[Zr(OEP)(OETAP)][Gd(OETAP)_2]$	1×10^{-7}	0.61
$Gd(OETAP)_2$	$\leq 5 \times 10^{-9}$	
$Zr(OEP)_2$	$\leq 5 \times 10^{-9}$	

what appears to be a general phenomenon has been offered by Kahn and Guillou.[32]

Similar to the above results, in $Gd(OETAP)_2$, the interaction between the $S = {}^7/_2$ Gd(III) center and the $S = {}^1/_2$ porphyrin π-radical is ferromagnetic in nature. This ferromagnetic interaction gives rise to an $S = 4$ ground state and an $S = 3$ excited state. As the temperature is decreased from 300 K, the $S = 3$ state is progressively depopulated, and $\chi_M T$ gradually approaches the value expected for ferromagnetically coupled $S_1 = {}^7/_2$ and $S_2 = {}^1/_2$ spins [$\chi_M T = S(S + 1)/2 = 10$]. At 5 K, $\chi_M T$ is equal to 10 cm^3 K mol^{-1}, and only the $S = 4$ state is populated. The calculated value of J (+1.9 cm^{-1}) indicates a weak ferromagnetic interaction and compares well with the values obtained earlier for Gd(III)−nitroxide systems[30] and for Gd(III)−Cu(II) pairs.[29,31,32] The existence of this ferromagnetic interaction in $Gd(OETAP)_2$ confirms the view that it is a general phenomenon in molecular species containing a Gd(III) ion in the proximity of an unpaired spin. It also corroborates the Kahn−Guillou explanation that the extremely weak delocalization of the 4f orbitals toward the ligand orbitals (here the porphyrin π orbitals) results in zero overlap density and a vanishing *intramolecular* antiferromagnetic contribution.[32] On the other hand, the decrease of $\chi_M T$ below 5 K may indicate weak *intermolecular* antiferromagnetic interactions between the ferromagnetic $Gd(OETAP)_2$ units.

In contrast, $[Zr(OEP)_2][Gd(OETAP)_2]$ behaves like a simple paramagnet, and it follows the Curie law in the temperature range of 7−300 K. The experimental value of $\chi_M T$ for this compound is close to the theoretical value expected for two noninteracting $S_1 = {}^7/_2$ and $S_2 = {}^1/_2$ spins {$\chi_M T = [S_1(S_1 + 1)/2] + [S_2(S_2 + 1)/2] = 8.25$ cm^3 K mol^{-1}}. There is no noticeable increase of $\chi_M T$ as the sample is cooled to about 7 K, indicating that any ferromagnetic interaction between the cationic and anionic units is too weak to be detected. The absence of any noticeable ferromagnetic interaction between the $S_1 = {}^7/_2$ spin on the anion and the $S_2 = {}^1/_2$ spin on the cation is very likely related to their distant locations on distinct molecular units within the solid lattice, as well as to the absence of any connecting framework that could provide a pathway for their interaction.

Conductivity Measurements

Two-probe conductivity measurements were performed on pressed pellets of crystals of the three charge-transfer systems. The results of several repeated conductivity measurements are presented in Table 4 and are compared to those for the undoped $Gd(OETAP)_2$ and $Zr(OEP)_2$ complexes.

The conductivities of the three charge-transfer systems are at least 2−4 orders of magnitude higher than the conductivities of the undoped molecules. We can provide only an upper limit on the values for the undoped sandwiches because they fell below the lower limits of our instrument. Although there is a significant increase compared to the conductivity of the undoped sandwiches, the conductivities of the charge-transfer systems are only in the lower semiconducting region.

Conductivity can be expressed with the general equation

$$\sigma = ne\mu \tag{1}$$

where σ is the conductivity, n is the number of carriers, e is the carrier charge, and μ is the carrier mobility. The number of carriers in charge-transfer complexes depends on the degree of charge transfer. It is not surprising that [Zr(OEP)(OETAP)][Gd(OETAP)$_2$], which has only a small amount of charge transfer, has the lowest conductivity of the three systems.

The low conductivity values indicate weak intermolecular overlap and an inefficient conductivity pathway, giving rise to a low mobility (eq 1). Insight into the low conductivity of these systems can be found from the crystal structure of $Zr(OEP)_2$.[10] Because the porphyrin rings are held closer together than their van der Waals distance, they are severely deformed into domes facing away from each other. This deviation from planarity diminishes the potential for intermolecular overlap. The ethyl groups may further prevent close interaction of the porphyrins. Without an efficient pathway for carrier propagation through the material, lower conductivity values result.

Pressed-pellet conductivity measurements of $[Ti(Pc)_2][I_2]$ and $[Sn(Pc)_2][I_2]$ (Pc = phthalocyanine) produced conductivities of 10^{-3} and 10^{-2} Ω^{-1} cm^{-1}, respectively.[3] Thin films of $[Lu(Pc)_2][DDQ_{0.6}]$ showed a conductivity of 5×10^{-3} Ω^{-1} cm^{-1}.[4] In both of these cases, the phthalocyanine sandwiches are more highly conducting than the porphyrin sandwiches discussed in this paper, possibly because they do not have ethyl groups, which prevent close approach of the macrocycle faces. However, the phthalocyanine sandwiches have diminished conductivity compared to flat monophthalocyanines such as $[Ni(II)Pc][I_3]_{1/3}$, which shows a conductivity of 10^2-10^3 Ω^{-1} cm^{-1}.[5] Therefore, doming affects the conductivity of the phthalocyanine sandwich complexes as well.

In the absence of a crystal structure, we cannot rule out structural factors other than doming that would lead to a low conductivity (such as the orientation of the sandwich complexes relative to each other) in the charge-transfer systems presented in this work. The weak intermolecular interactions of the sandwiches do indicate that the porphyrin charge-transfer systems have conductivity that can be best described as localized charges that hop from site to site.

The charge-transfer systems followed thermally activated conductivity, and their conductivity was fit to eq 2.

$$\sigma = \sigma_o \exp(-E_{act}/2kT) \tag{2}$$

In eq 2, σ is the conductivity, σ_o is a constant, E_{act} is the thermal activation barrier to conductivity (with all the contributing factors combined into one term), k is the Boltzmann constant, and T is the temperature. The value of the slope of a plot of $-\ln(\sigma)$ vs ${}^1/_2kT$ gives the activation energies, which are presented in Table 4 for the three charge-transfer species.

Conclusion

Lanthanide(III) bis(porphyrin) sandwich complexes of gadolinium and lutetium were synthesized from OETAP. The reduced, protio [Ln(OETAP)$_2$H] and the π-radical [Ln(OETAP)$_2$] forms were distinguished by UV−vis, near-IR, and IR spectroscopies. Predictably, the $Ln(OETAP)_2$ complexes are very easily reduced. The $Ln(OETAP)_2$ compounds were reacted with zirconium(IV) bis(porphyrin) sandwiches to form charge-transfer complexes in which the zirconium(IV) sandwiches were

partially oxidized by the lanthanide(III) sandwiches. The solution charge-transfer properties of these systems were studied in a number of solvents. No precipitate formed in any of the charge-transfer reactions because of the high solubility of the sandwiches and the destabilization of the charge-transfer products in the less polar solvents (from which a charged species would more likely precipitate).

Crystals of the charge-transfer species were grown as materials for solid-state studies. Magnetic studies indicated the presence of noninteracting spins between the $S = {}^1/_2$ π electron undergoing the charge transfer and the $S = {}^7/_2$ Gd(III) electrons, indicating weak intermolecular interactions. Conductivity studies showed that, whereas the lanthanide and zirconium sandwiches themselves are insulators, the charge-transfer materials are semiconductors. However, the low conductivities for the charge-transfer materials are consistent with weakly interacting systems. Strong intermolecular interactions are perhaps prevented by the presence of ethyl substituents and the distortion of the porphyrin rings in the sandwich complexes.

Acknowledgment. We thank Dr. Paul Rey for his help with the magnetic susceptibility fits and for several helpful discussions. We thank Prof. Gordon Brown, Prof. Henry Taube, Prof. William A. Little, Prof. Noel Hush, Dr. M. J. Holcomb, and Dr. T. A. Eberspacher for helpful discussions. This work was supported financially by the NSF (Grant CHE 9123187-A4).

Supporting Information Available: Infrared spectra of Gd(OETAP)$_2$ and Gd(OETAP)$_2$H. This material is available free of charge via the Internet at http://pubs.acs.org.

IC9907516